

SCIENTIFIC REPORTS



OPEN

MART-10 represses cholangiocarcinoma cell growth and high vitamin D receptor expression indicates better prognosis for cholangiocarcinoma

Received: 13 October 2016

Accepted: 30 January 2017

Published: 03 March 2017

Kun-Chun Chiang^{1,2,*}, Ta-Sen Yeh^{3,*}, Cheng-Cheng Huang⁴, Yu-Chan Chang⁵, Horng-Heng Juang⁶, Chi-Tung Cheng³, Jong-Hwei S. Pang⁷, Jun-Te Hsu³, Masashi Takano⁸, Tai C. Chen⁹, Atsushi Kittaka⁸, Michael Hsiao⁵ & Chun-Nan Yeh³

Cholangiocarcinoma (CCA) is a devastating disease due to no effective treatments available. Since the non-mineral functions of vitamin D emerges, $1\alpha,25(\text{OH})_2\text{D}_3$, the active form of vitamin D, has been applied in anti-cancer researches. In this study, we demonstrated that both the $1\alpha,25(\text{OH})_2\text{D}_3$ analog, MART-10, and $1\alpha,25(\text{OH})_2\text{D}_3$ possessed anti-growth effect on human CCA cells with MART-10 much more potent than $1\alpha,25(\text{OH})_2\text{D}_3$. The growth inhibition of both drugs were mediated by induction of G0/G1 cell cycle arrest through upregulation of p27 and downregulation of CDK4, CDK6, and cyclin D3. Human neutrophil gelatinase associated lipocalin (NGAL) was found to be involved in $1\alpha,25(\text{OH})_2\text{D}_3$ and MART-10 mediated growth inhibition for CCA as knockdown of NGAL decreased Ki-67 expression in SNU308 cells and rendered SNU308 cells less responsive to $1\alpha,25(\text{OH})_2\text{D}_3$ and MART-10 treatment. Vitamin D receptor (VDR) knockdown partly abolished MART-10-induced inhibition of NGAL and cell growth in SNU308 cells. The xenograft animal study demonstrated MART-10 could effectively repressed CCA growth *in vivo* without inducing obvious side effects. The IHC examination of human CCA specimen for VDR revealed that higher VDR expression was linked with better prognosis. Collectively, our results suggest that MART-10 could be a promising regimen for CCA treatment.

Cholangiocarcinoma (CCA) accounts for 10–15% of primary liver cancers and is the second most common primary liver cancer after hepatocellular carcinoma. It is estimated that 1/100000 people are diagnosed of CCA per year in the western countries^{1–4}. Of note, the incidence and mortality of CCA has increased in the recent years^{5,6}. CCA is generally with poor response to traditional chemotherapy and radiotherapy. So far, radical surgery resection remains the best choice of treatment for CCA whenever feasible^{7–9}. However, the high recurrent rate after resection and delay diagnosis, which makes most CCA patients not good candidates to receive surgery, lead to poor prognosis¹⁰. In general, only 25–30% of CCA patients would receive surgery^{11,12}. Regarding patients with unresectable CCA, prognosis is very dismal with most of them having survival less than 1 year¹³. Thus, to develop a new treatment against CCA should be prioritized.

¹General Surgery Department, Chang Gung Memorial Hospital, Chang Gung University, Keelung, R.O.C, Taiwan. ²Director of Zebrafish center of Keelung Chang Gung Memorial Hospital, R.O.C, Taiwan. ³General Surgery Department and Liver research center, Chang Gung Memorial Hospital, Chang Gung University, Kwei-Shan, Taoyuan, R.O.C, Taiwan. ⁴Department of Pathology, Chang Gung Memorial Hospital, 222, Mai-Chin Road, Keelung, R.O.C, Taiwan. ⁵Genomics Research Center, Academia Sinica, Taipei, R.O.C, Taiwan. ⁶Department of Anatomy, College of Medicine, Chang Gung University, Kwei-Shan, Taoyuan, 333, R.O.C, Taiwan. ⁷Graduate Institute of Clinical Medical Sciences, College of Medicine, Chang Gung University, Kwei-Shan, Taoyuan, R.O.C, Taiwan. ⁸Faculty of Pharmaceutical Sciences, Teikyo University, Sagami-hara, Kanagawa, 252-5195, Japan. ⁹Boston University School of Medicine, M-1022, 715 Albany Street, Boston, MA 02118, USA. *These authors contributed equally to this work. Correspondence and requests for materials should be addressed to H.-H.J. (email: hhj143@mail.cgu.edu.tw) or M.H. (email: mhsiao@gate.sinica.edu.tw) or C.-N.Y. (email: yehchunna@gmail.com)

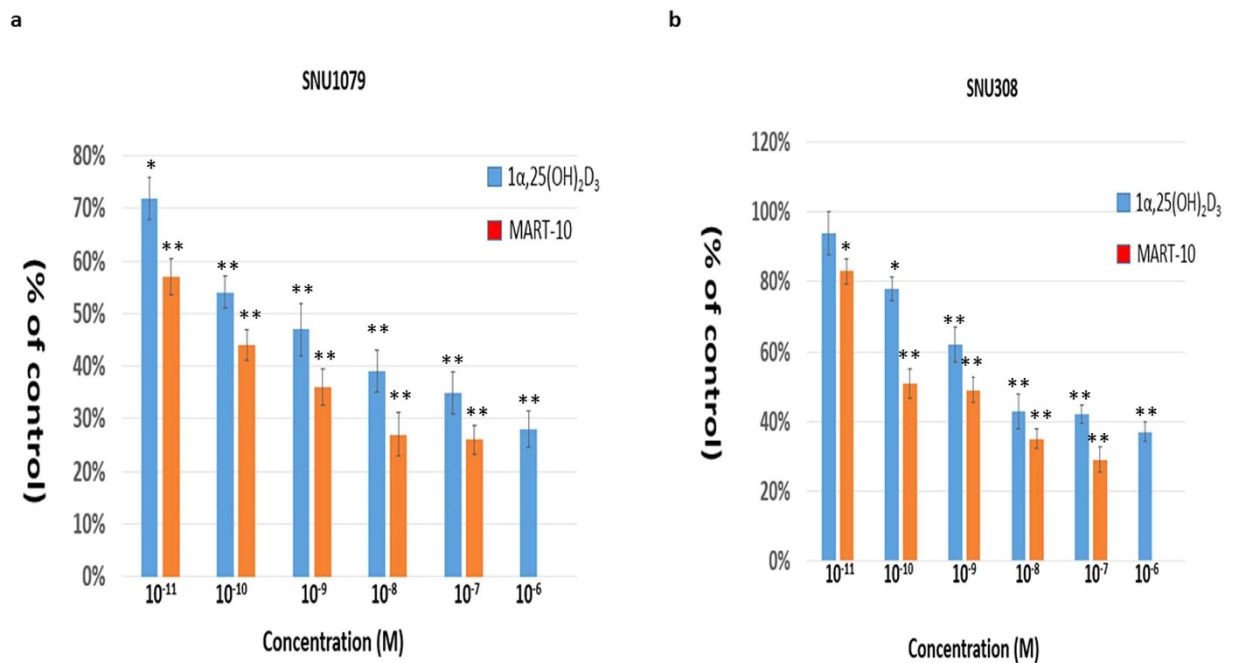


Figure 1. Anti-proliferative effects of $1\alpha,25(\text{OH})_2\text{D}_3$ and MART-10 on CCA cells. Two, four, and six days after plating, cells were treated with $1\alpha,25(\text{OH})_2\text{D}_3$ or MART-10 with indicated concentrations. The cell proliferation was measured by WST-1 method. (a) Both $1\alpha,25(\text{OH})_2\text{D}_3$ and MART-10 inhibited SNU1079 cell proliferation dose-dependently with MART-10 much more potent than $1\alpha,25(\text{OH})_2\text{D}_3$. (b) SNU308 cell proliferation was repressed by $1\alpha,25(\text{OH})_2\text{D}_3$ or MART-10 in a dose-dependent manner. MART-10 was more effective than $1\alpha,25(\text{OH})_2\text{D}_3$. Each value is a mean \pm SD of three to five determinations. * $p < 0.05$, ** $p < 0.01$ versus control.

Since the non-mineral functions of vitamin D has been discovered during the past decades, mainly consisting of pro-differentiation, pro-apoptosis, anti-angiogenesis, etc., vitamin D has emerged as a new regimen against cancer growth and abundances of studies have been published regarding vitamin D application for cancer treatment^{14–16}. For clinical application, thousands of $1\alpha,25(\text{OH})_2\text{D}_3$ (the active form of vitamin D) analogs have been synthesized to minimize the side effect of hypercalcemia and to strengthen other effects, mainly the anti-tumor growth effect¹⁷. To modulate gene expression, $1\alpha,25(\text{OH})_2\text{D}_3$ needs to bind with vitamin D receptor (VDR), which further conjugates with RXR to form a heterodimer¹⁸. As genes with vitamin D response elements (VDRE) within the promoter area, these genes are subject to $1\alpha,25(\text{OH})_2\text{D}_3$ -VDR-RXR complex modulation¹⁹. So far, at least 693 genes have been found to be $1\alpha,25(\text{OH})_2\text{D}_3$ responsive²⁰. Since VDR has been found to exist in a variety of cancer cell lines, it is not surprising that a lot of cancer cells growth are inhibited by $1\alpha,25(\text{OH})_2\text{D}_3$ ^{16,21–25}. For CCA, overexpression of VDR has been linked to a better prognosis for CCA patients and 22-oxa-1,25-dihydroxyvitamin D₃, one kind of $1\alpha,25(\text{OH})_2\text{D}_3$ analog, has been shown to be able to repress CCA cell growth *in vitro* and *in vivo*^{26,27}. In addition, oral supplementation of vitamin D could effectively prevent CCA occurrence and inhibit growth in a chemical-induced rat CCA model²⁸. Collectively, application of vitamin D and its analogs to treat CCA seems to be a promising way for CCA treatment under current bleak background.

MART-10 (19-nor-2α-(3-hydroxypropyl)- $1\alpha,25(\text{OH})_2\text{D}_3$)²⁹, which has 19-nor structure and A-ring modification at C2 position, has been shown by our group to inhibit a variety of cancer cell growth and metastasis^{21,25,30–34} and to be effective and safe in a pancreatic cancer cell xenograft animal model³⁵.

Lipocalin-2 (LCN2), known as NGAL as well, is a secreted protein. After secretion, NGAL functions not only as a transporter for some substances and also interacting with other ligands, thus involved in lots of important physiological functions^{36,37}. NGAL has also been found to play as an oncogene in a myriad of cancers³⁸, though some controversies exist^{39–41}.

In this study, we aimed to investigate the feasibility of applying MART-10 to treat CCA *in vitro* and *in vivo* and the effect of MART-10 on NGAL expression in CCA. In addition, we would also investigate the relationship between VDR expressions and clinicopathological features of CCA patients to further justify vitamin D and its analogs application in CCA treatment.

Result

Anti-proliferative effect of MART-10 and $1\alpha,25(\text{OH})_2\text{D}_3$ on SNU308 and SNU1079 cells. Figure 1a shows that $1\alpha,25(\text{OH})_2\text{D}_3$, from 10⁻⁶ to 10⁻¹¹ M, and MART-10, from 10⁻⁷ to 10⁻¹¹ M, significantly inhibited SNU1079 cell proliferation after 7 days of treatment as determined by WST-1 method. Regarding SNU308 cells, 10⁻⁷ to 10⁻¹⁰ M $1\alpha,25(\text{OH})_2\text{D}_3$ and 10⁻⁷ to 10⁻¹¹ M MART-10 could effectively attenuate

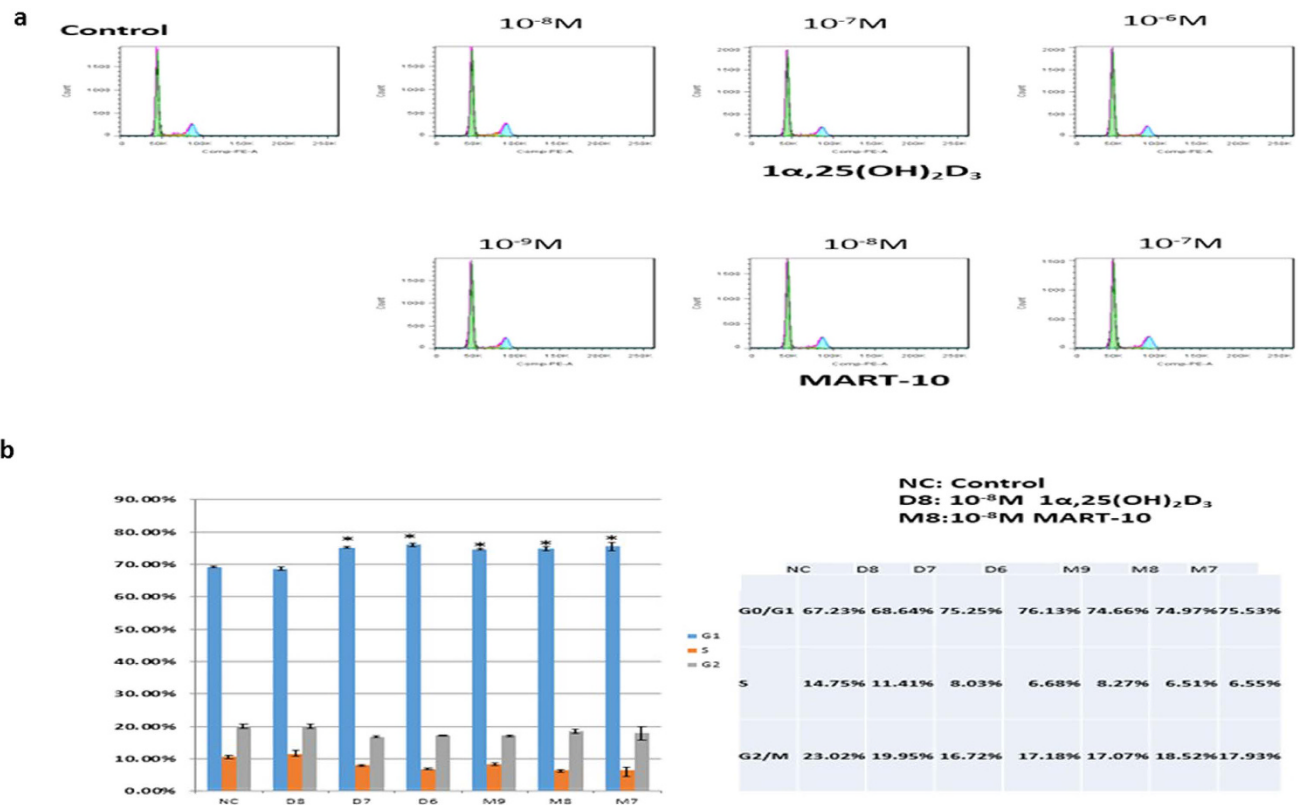


Figure 2. Flow cytometry analysis of cell cycle distribution for SNU308 cells after 1α,25(OH)₂D₃ or MART-10 treatment. SNU308 cells were treated with 1α,25(OH)₂D₃ from 10⁻⁸ M to 10⁻⁶ or MART-10 from 10⁻⁹ M to 10⁻⁷ M for two days and then analyzed by flow cytometry. (a) A representative DNA histogram for control, 1α,25(OH)₂D₃- or MART-10-treated SNU308 cells. The total DNA amount of cells (x-axis) was obtained by staining cells with propidium iodide. (b) The quantitative result of SNU308 cell cycle distribution with or without treatment. Both 1α,25(OH)₂D₃ and MART-10 induced G₀/G₁ arrest in SNU308 cells. (*p < 0.05).

cell proliferation (Fig. 1b). Our data clearly indicate that both MART-10 and 1α,25(OH)₂D₃ could significantly inhibit CCA cells proliferation with MART-10 much more potent than 1α,25(OH)₂D₃.

Induction of cell cycle arrest at G₀/G₁ phase by MART-10 and 1α,25(OH)₂D₃ in SNU308 cells. To further understand the growth inhibition mechanisms mediated by MART-10 and 1α,25(OH)₂D₃ in CCA cells, we then conducted cell cycle analysis to evaluate the cell cycle distribution by flow cytometry after two days of 1α,25(OH)₂D₃ or MART-10 treatment. As shown in Fig. 2, SNU308 cells were treated by 1α,25(OH)₂D₃ or MART-10 at concentrations ranging from 10⁻⁸ to 10⁻⁶ or 10⁻⁹ to 10⁻⁷ M, respectively. Our data suggest that both 1α,25(OH)₂D₃ and MART-10 could induced cell cycle arrest at G₀/G₁ phase in SNU308 cells, leading to the growth inhibition shown in Fig. 1.

Evaluation of apoptosis induction of 1α,25(OH)₂D₃ and MART-10 in SNU308 cells. To evaluate whether 1α,25(OH)₂D₃ or MART-10 treatment could induce apoptosis in CCA cells or not, we thus conducted TUNEL assay after two days of 1α,25(OH)₂D₃ or MART-10 treatment. As shown in Fig. 3, neither 1α,25(OH)₂D₃ nor MART-10 would induce apoptosis in SNU308 cells.

Evaluation of CDK inhibitors of p21 and p27 expression in SNU308 cells by 1α,25(OH)₂D₃ and MART-10. To further clarify the mechanisms by which 1α,25(OH)₂D₃ and MART-10 arrest CCA cell cycle progression at G₀/G₁ phase, the expression of the two main cyclin dependent kinase (CDK) inhibitors, p21 and p27, responsible for G₀/G₁ arrest, were examined by western blot analysis (Fig. 4). The quantitative result of western blot revealed that p27 was upregulated by 10⁻⁶ to 10⁻⁸ 1α,25(OH)₂D₃ and 10⁻⁷ to 10⁻⁹ M MART-10 in a dose dependent manner. As for p21 expression, neither 1α,25(OH)₂D₃ nor MART-10 had significant impact in SNU308 cells. Collectively, our result demonstrates that both 1α,25(OH)₂D₃ and MART-10 could increase p27 expression SNU308 cells, but not p21, resulting into the G₀/G₁ cell cycle arrest noted in Fig. 2.

Evaluation of Cyclin D3, CDK4, CDK6 expression in SNU308 cells after 1α,25(OH)₂D₃ or MART-10 treatment. We next evaluated CDK4, CDK6, cyclin D3, which are all important elements for cells to pass through G₁/S transition checkpoints, expressions in SNU308 cells after two days treatment. As shown in Fig. 5, 1α,25(OH)₂D₃ significantly inhibited CDK4, CDK6, and cyclin D3 expressions at 10⁻⁶ and 10⁻⁷ M in SNU308 cells; while MART-10, at 10⁻⁷, 10⁻⁸, and 10⁻⁹ M repressed CDK4, CDK6, and cyclin D3 expressions to

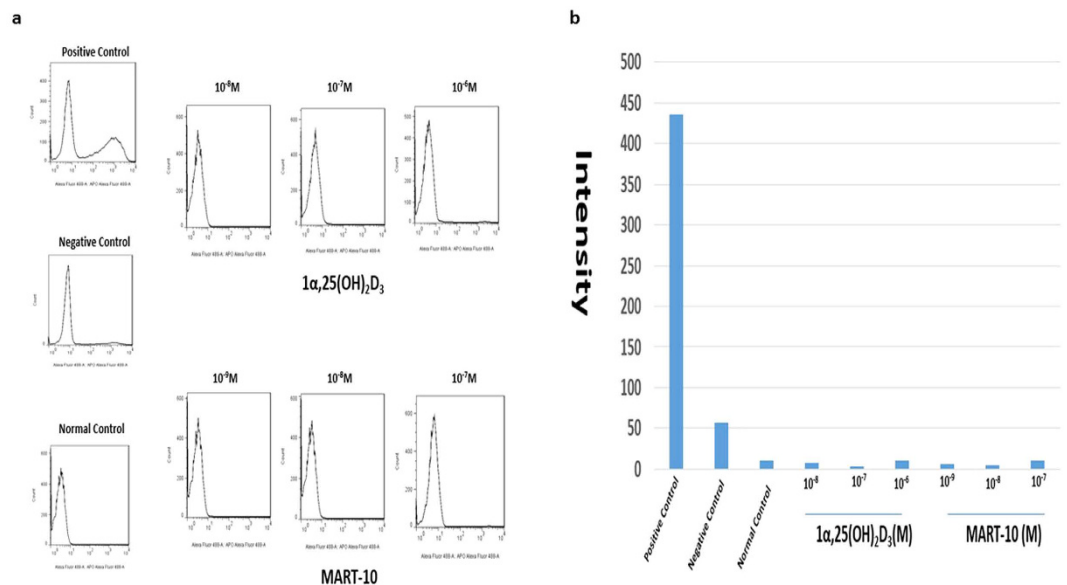


Figure 3. TUNEL assay and Flow cytometry analysis for apoptosis induction in SNU308 cells by 1α,25(OH)₂D₃ and MART-10. After two days of treatment, SNU308 cells were stained by APOTM-BrdU TUNEL kit and analyzed by flow cytometry to detect apoptosis induction. Our result indicates that neither 1α,25(OH)₂D₃ nor MART-10 would induce apoptosis in SNU308 cells.

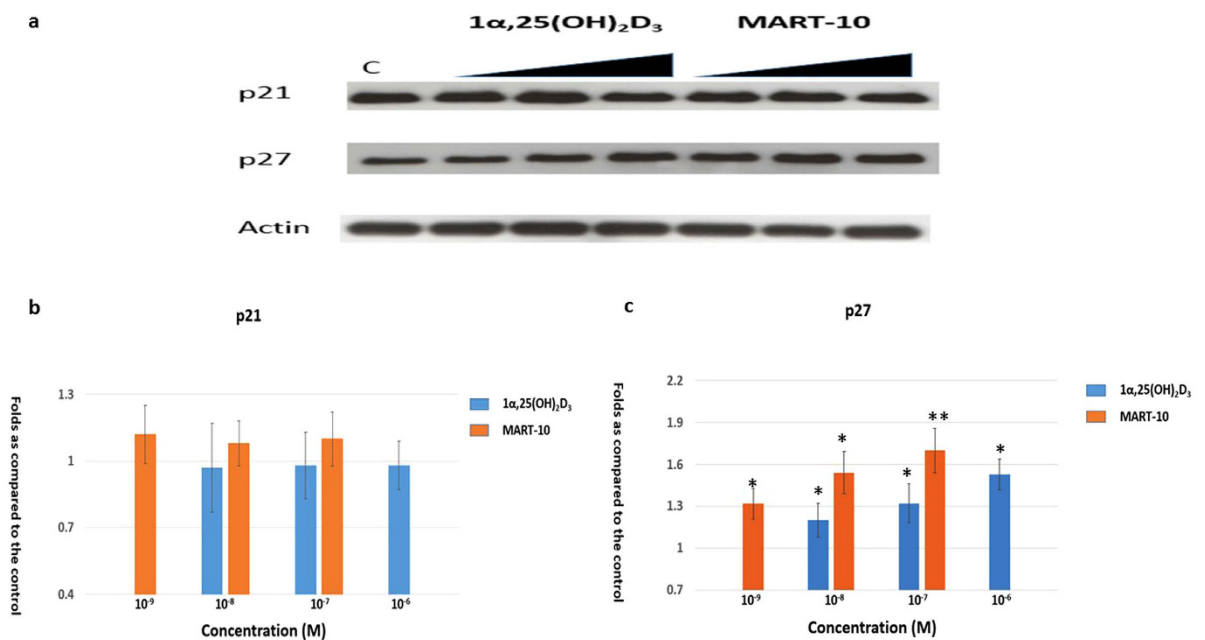


Figure 4. Evaluation of 1α,25(OH)₂D₃ and MART-10 effect on p21 and p27 expressions in SNU308 cells. After two days of treatment (10⁻⁶ to 10⁻⁸ 1α,25(OH)₂D₃ or 10⁻⁷ to 10⁻⁹ M MART-10), p21 and p27 expressions were determined by western blot. (a) A western blot showing p21 and p27 expression in SNU308 cells with or without treatment. Actin was used as the loading control. (cropped). (b) Quantitative result of western blot. Both 1α,25(OH)₂D₃ and MART-10 increased p27 expression in SNU308 cells without obvious effect on p21. MART-10 was more effective than 1α,25(OH)₂D₃. Each value is a mean ± SD of three to five determinations. *p < 0.05, **p < 0.01 versus control.

the greater extent as compared to 1α,25(OH)₂D₃ (Fig. 5). Thus, we concluded that SNU308 cell cycle arrest at G0/G1 as induced by 1α,25(OH)₂D₃ and MART-10 were also mediated by inhibition of CDK4, CDK6, and cyclin D3 expression in addition to upregulation of p27.

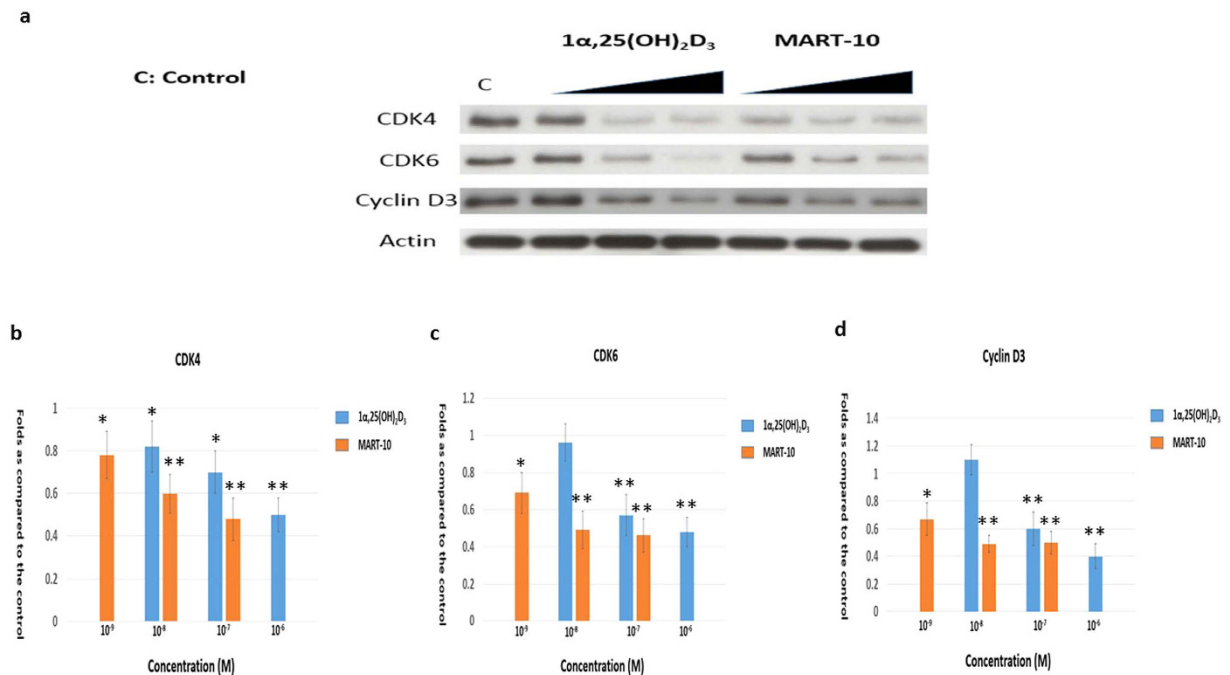


Figure 5. Evaluation of 1 α ,25(OH) $_2$ D $_3$ and MART-10 effect on CDK4, CDK6, and cyclin D3 expressions in SNU308 cells. After two days of treatment (10⁻⁶ to 10⁻⁸ 1 α ,25(OH) $_2$ D $_3$ or 10⁻⁷ to 10⁻⁹ M MART-10), CDK4, CDK6 and cyclin D3 expressions were determined by western blot. **(a)** A western blot showing CDK4, CDK6 and cyclin D3 expression in SNU308 cells with or without treatment. Actin was used as the loading control. (cropped). **(b)** Quantitative result of western blot. Both 1 α ,25(OH) $_2$ D $_3$ and MART-10 decreased CDK4, CDK6 and cyclin D3 expression in SNU308 cells with MART-10 more effective than 1 α ,25(OH) $_2$ D $_3$. Each value is a mean \pm SD of three to five determinations. **p* < 0.05, ***p* < 0.01 versus control.

Evaluation of 1 α ,25(OH) $_2$ D $_3$ and MART-10 effect on NGAL expression in SNU308 cells. Previously, we have shown NGAL expression in CCA cells and knockdown of NGAL in CCA cells was able to increase CCA cells doubling time, indicating NGAL role as an oncogene in human CCA²⁸. We thus investigated NGAL expression after 1 α ,25(OH) $_2$ D $_3$ or MART-10 treatment in SNU308 cells. As shown in Fig. 6a and b, a dose dependent manner of inhibition of NGAL in SNU308 cells was observed for 10⁻⁶ and 10⁻⁷ M 1 α ,25(OH) $_2$ D $_3$ and 10⁻⁷, 10⁻⁸, and 10⁻⁹ M MART-10 with MART-10 much more potent than 1 α ,25(OH) $_2$ D $_3$.

Evaluation of NGAL effect on Ki-67 expression in SNU308 cells. To further prove the oncogene role of NGAL for human CCA, we next measured Ki-67 expressions in SNU308 cells and SNU308-NGALsi cells by flow cytometry. As shown in Fig. 6c and d, Ki-67 expression in SNU308-NGALsi cells is about 0.56 fold to that of SNU308 cells, implying the oncogene role of NGAL in human CCA and consistent with our previous study²⁸.

Evaluation of 1 α ,25(OH) $_2$ D $_3$ and MART-10 effect on SNU308 cells and SNU308-NGALsi cells growth. Since NGAL is one of the 1 α ,25(OH) $_2$ D $_3$ and MART-10 responsive gene in snu308 cells, to further understand NGAL role in 1 α ,25(OH) $_2$ D $_3$ or MART-10 mediated growth inhibition in human CCA cells, we thus treated SNU308-NGALsi cells with 1 α ,25(OH) $_2$ D $_3$ or MART-10 and compared the result with that shown in Fig. 1b. As shown in Fig. 6e, 10⁻⁶, 10⁻⁷, and 10⁻⁸ M 1 α ,25(OH) $_2$ D $_3$ and 10⁻⁷ to 10⁻¹¹ M MART-10 could effectively repress SNU308-NGALsi cell growth as determined by WST1 method; however, the inhibition effect was much less than that observed in SNU308 cells shown in Fig. 1b. We further applied recombinant human NGAL (rhNGAL) to treat SU308 and SNU308NGAL-si cells. Figure 6f shows that the cell growth of SU308 and SNU308NGAL-si cells were increased by rhNGAL. MART-10 effectively repressed rhNGAL-increased cell growth in both kinds of cells. Our data suggests that the growth inhibition for CCA cells by 1 α ,25(OH) $_2$ D $_3$ or MART-10 is partly mediated by NGAL inhibition.

Evaluation of VDR role in MART-10-induced inhibition of NGAL expression and cell growth in CCA cells. To investigate how MART-10 influenced NGAL expression in CCA cells, we then knocked down VDR in SNU308 cells (SNU308-VDRsi). As shown in Fig. 7a, SNU308-VDRsi cells expressed much weaker VDR expression than SNU308-COLsi cells (mock knockdown of VDR). SNU308-COLsi and SNU308-VDRsi cells were further treated by 10⁻⁸ and 10⁻⁹ M MART-10 for 7 days and the proliferation of SNU308-VDRsi cells were inhibited to 64% and 82% as compared to SNU308-COLsi cells (Fig. 7b). NGAL expression in SNU308 cells was not influenced significantly by MART-10 after VDR knockdown (Fig. 7c). The reporter assay indicated that NGAL reporter activity was repressed by MART-10 in a dose dependent manner (Fig. 7d) and NGAL reporter

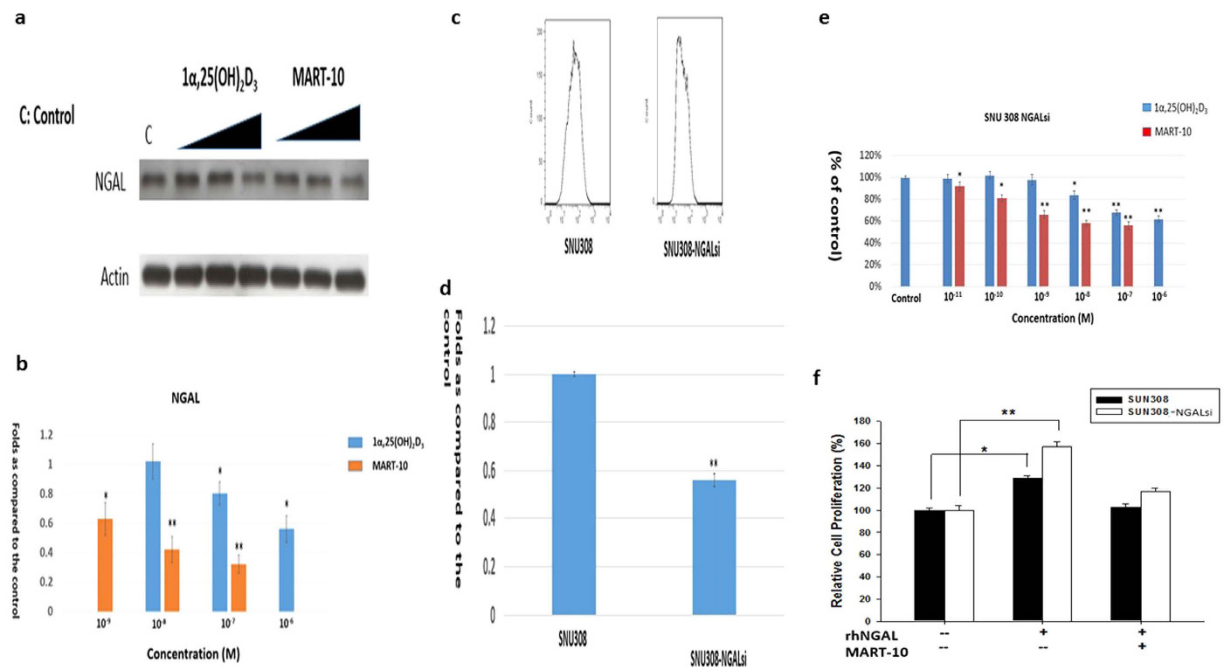


Figure 6. Evaluation of $1\alpha,25(\text{OH})_2\text{D}_3$ and MART-10 effect on NGAL expression in SNU308 cells and proliferation on SNU308 and SNU308-NGALsi cells, and NGAL effect on ki-67 expression of SNU308 cells. NGAL expression in SNU308 cells was evaluated by western blot after two days of 10^{-6} to 10^{-9} $1\alpha,25(\text{OH})_2\text{D}_3$ or 10^{-7} to 10^{-9} M MART-10 treatment. (a) A western blot depicting NGAL expression in SNU308 cells with or without treatment. Actin was used as the loading control. (cropped). (b) Quantitative result of western blot. Both $1\alpha,25(\text{OH})_2\text{D}_3$ and MART-10 repressed NGAL expression in SNU308 cells with MART-10 more effective than $1\alpha,25(\text{OH})_2\text{D}_3$. To investigate NGAL role in SNU308 cells, Ki-67 expression was measured by flow cytometry in SNU308 cells and SNU308 NGAL-si cells. (c) The histogram of Ki-67 expression in SNU308 cells and SNU308 NGAL-si cells. (d) The quantitative result of Ki-67 expression in SNU308 cells and SNU308 NGAL-si cells. Our result indicates that knockdown of NGAL in SNU308 cells decreased Ki-67 expression. (e) SNU308NGAL-si cells were treated by $1\alpha,25(\text{OH})_2\text{D}_3$ or MART-10 as indicated concentrations every two days. 7 days later, the cell proliferation was measured by WST-1 method. Both $1\alpha,25(\text{OH})_2\text{D}_3$ and MART-10 inhibited SNU308 NGAL-si cells proliferation dose-dependently with MART-10 much more potent than $1\alpha,25(\text{OH})_2\text{D}_3$. However, the inhibition effect was less than that observed in SNU308 cells. (f) SNU308 and SNU308NGAL-si cells were treated by either vehicle, or rhNGAL (0.5 ng/ml), or rhNGAL and MART-10. The cell proliferation was measured two days later. rhNGAL increased cell growth of both SNU308 and SNU308NGAL-si cells. The rhNGAL-increased cell growth was abolished by MART-10. (Each value is a mean \pm SD of three to five determinations. * $p < 0.05$, ** $p < 0.01$ versus control).

activity was less inhibited by MART-10 as VDR knockdown (Fig. 7e). Based on our result, MART-10 induced NGAL inhibition and MART-10 repressed CCA cell growth partly VDR-dependently.

Evaluation of $1\alpha,25(\text{OH})_2\text{D}_3$ and MART-10 on CCA cell growth *in vivo*. To evaluate the effectiveness and safety of application of $1\alpha,25(\text{OH})_2\text{D}_3$ and MART-10 *in vivo*, we next xenografted SNU308 cells in mice and treated them with or without $1\alpha,25(\text{OH})_2\text{D}_3$ (0.3 $\mu\text{g}/\text{kg}$) or MART-10 (0.15 $\mu\text{g}/\text{kg}$ or 0.3 $\mu\text{g}/\text{kg}$) two times a week. The tumor volume, body weight and serum calcium were checked every week. As shown in Fig. 8b and c, both $1\alpha,25(\text{OH})_2\text{D}_3$ and MART-10 could significantly repress SNU308 cells growth *in vivo* with MART-10 much more potent than $1\alpha,25(\text{OH})_2\text{D}_3$. The stable body weight and normal serum calcium of mice during the study period indicated both $1\alpha,25(\text{OH})_2\text{D}_3$ and MART-10 are safe under the current applied doses (Fig. 8d and e).

Correlations between VDR expression and clinicopathological features in CCA patients undergoing hepatectomy. We next analyzed correlations between VDR expression levels and clinicopathological features of 79 CCA patients. Among specimens from 79 CCA patients who underwent hepatectomy, 44 (49.4%) specimens showed high VDR staining intensity (Fig. 9a). Of note, VDR upregulation strongly correlated with negative symptoms, negative lymph node metastasis and a negative resection margin (Supplemental Table 1).

Low VDR expression is a poor prognostic indicator for CCA patients undergoing hepatectomy. Univariate log-rank analysis was then applied to identify factors that had adverse influences on the overall survival (OS) rate in the aforementioned CCA patients. The presence of positive symptoms, elevated alkaline phosphatase level, elevated CEA levels, a tumor size >5 cm, a positive surgical-margin status and week

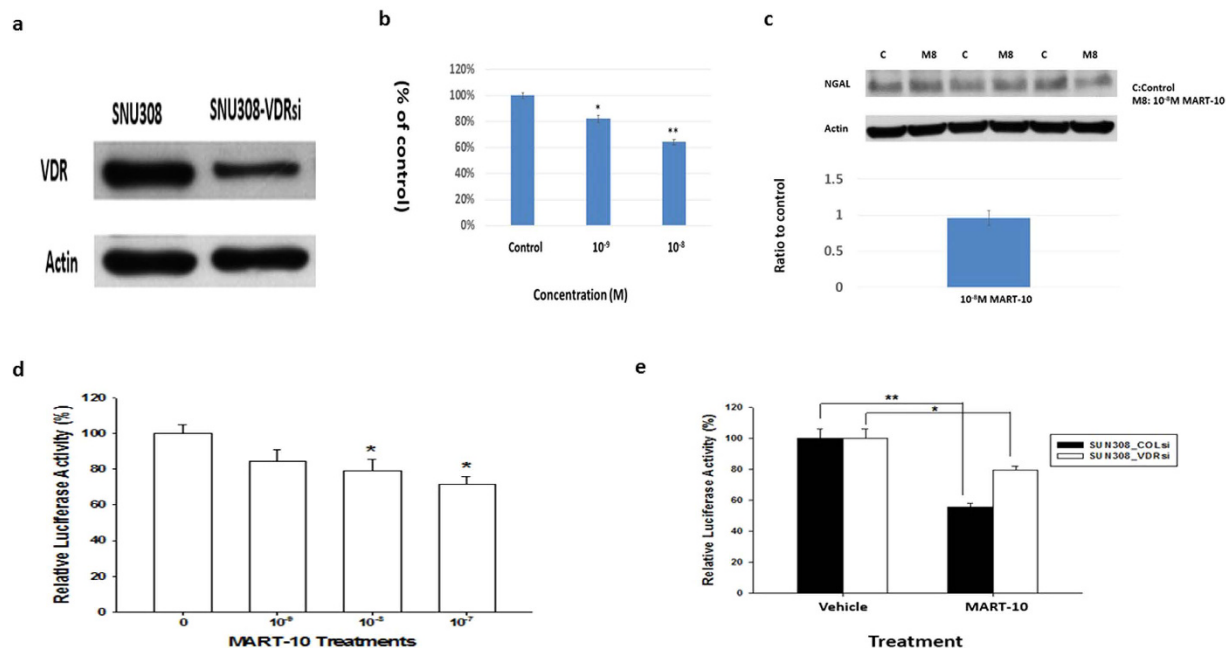


Figure 7. The role of VDR in MART-10-induced inhibition in cell growth and NGAL expression of CCA cells. (a) A western blot depicting VDR expression in SNU308-VDRsi (VDR knockdown) and SNU308-COLsi (mock knockdown) cells. Actin was used as the loading control. (cropped). (b) After 7 days of treatment, MART-10 repressed SNU308-VDRsi cell growth, which was less than that noted in SNU308 cells. (* $p < 0.05$, ** $p < 0.01$). (c) The NGAL protein expression in SNU308-VDRsi cells was not influenced by 10^{-8} M MART-10. (d) The NGAL reporter activity was inhibited by MART-10 in a dose dependent manner. (* $p < 0.05$). (e) VDR knockdown in SNU308 cells partly abolished MART-10-induced inhibition of NGAL reporter activity. (* $p < 0.05$ ** $p < 0.01$).

staining intensity were found to correlate with OS (Supplemental Table 2). However, only low VDR staining intensity was identified as independent predictors for an inferior OS rate in these patients after multivariate Cox proportional hazard analysis (Supplemental Table 3 and Fig. 9b).

Discussion

Since $1\alpha,25(\text{OH})_2\text{D}_3$ exerts its genomic functions through binding with vitamin D receptor (VDR) and 24-OHase (CYP24A1) is responsible for the degradation of $1\alpha,25(\text{OH})_2\text{D}_3$, the fact that MART-10 has higher VDR binding affinity⁴² and better resistance to CYP24A1-mediated degradation^{43,44} leads to the expectable higher VDR transactivation effect of MART-10 than $1\alpha,25(\text{OH})_2\text{D}_3$.

In this study, we showed that MART-10, a C-2 substituted, 19-nor analog of $1\alpha,25(\text{OH})_2\text{D}_3$, possessed much more potent anti-tumor growth effect on human CCA *in vitro* and *in vivo* through induction of cell cycle arrest at G0/G1 phase and inhibition of NGAL. The stable body weight and normal serum calcium concentration noted in the mice during the experiment period (Fig. 8d and e) indicate the safety and non-hypercalcemic characteristic of MART-10 *in vivo*. Since most genomic functions of $1\alpha,25(\text{OH})_2\text{D}_3$ are mediated through binding with VDR, the finding that high VDR expression in human CCA specimen is correlated with better prognosis (Fig. 9 and Supplemental Table 2) further encourages the application of MART-10 in clinical trial for advanced CCA patients.

Cells have to go through cell cycle progression to proliferate. Since cancer cells possess excess mitogenic signals, which lead to cell cycle dysregulation, cancer cells tend to have unlimited cell proliferation⁴⁵ and targeting cell cycle control becomes one important direction to attenuate cancer cell growth. Our data indicates that both $1\alpha,25(\text{OH})_2\text{D}_3$ and MART-10 could induce G0/G1 cell cycle arrest in SNU308 cells (Fig. 2) with MART-10 more potent than $1\alpha,25(\text{OH})_2\text{D}_3$, leading to the growth inhibition noted in Fig. 1.

The transcriptional factor E2F-1 needs to be active to drive cell through the restriction point to proceed cell cycle progression⁴⁶. However, E2F-1 is inactive in the beginning due to binding with hypophosphorylated retinoblastoma (RB)⁴⁷. To be active, specific cyclins and CDKs are needed to phosphorylate RB, which further releases E2F-1. Among others, CDK4, CDK6, and cyclin D3 are important proteins for RB phosphorylation, which are under negative control by CKIs p21 and p27. As shown in Fig. 4, both $1\alpha,25(\text{OH})_2\text{D}_3$ and MART-10 could upregulate p27 expression in SNU308 cells with MART-10 more effective. No obvious change of p21 expression was observed after treatment in SNU308 cells. In addition, CDK4, CDK6, and cyclin D3 were all downregulated as exposure to $1\alpha,25(\text{OH})_2\text{D}_3$ and MART-10 with the latter more potent (Fig. 5). Our data suggests that the induction of G0/G1 cell cycle arrest in SNU308 cells by $1\alpha,25(\text{OH})_2\text{D}_3$ and MART-10 is mediated by upregulation of p27 and downregulation of CDK4, CDK6, and cyclin D3.

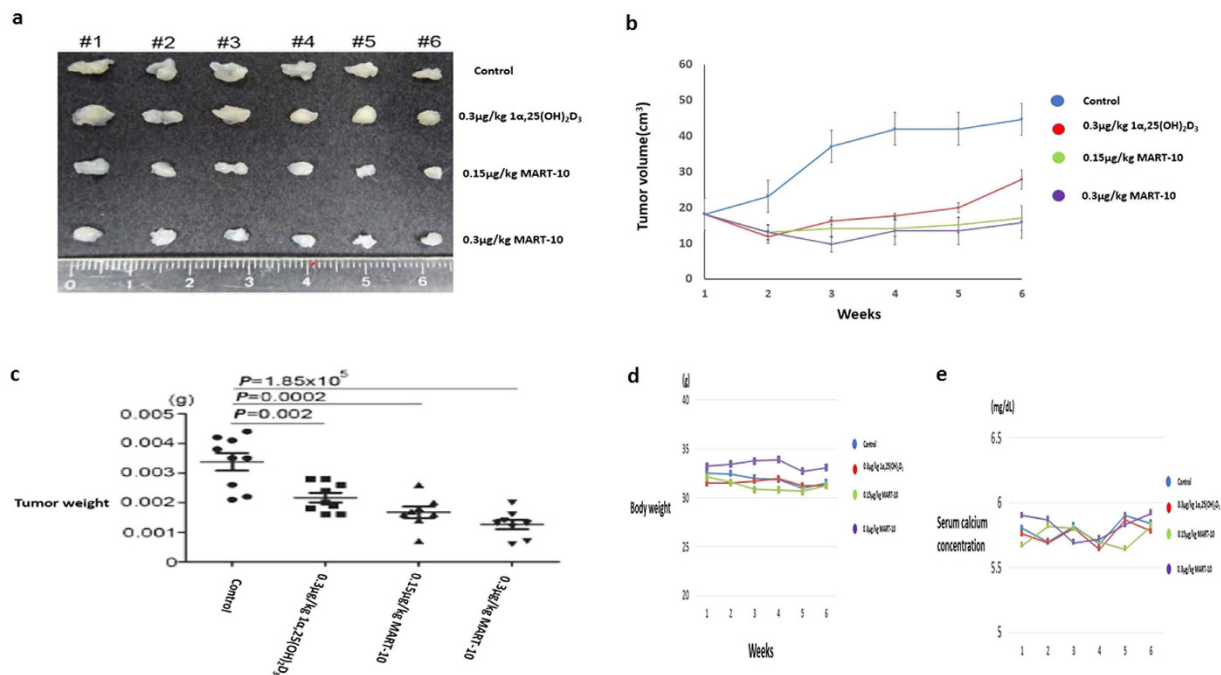


Figure 8. $1\alpha,25(\text{OH})_2\text{D}_3$ and MART-10 suppress SNU308 cell growth *in vivo* without obvious side effects. After 5 weeks of treatment (two times per week), the xenografted tumors were removed and the tumor weight was measured. Tumor volume, mice body weight and serum calcium were checked every week. **(a)** The photograph to show xenografted tumors from each group. **(b)** Tumor volume change as recorded every week. Both $1\alpha,25(\text{OH})_2\text{D}_3$ and MART-10 repressed xenografted tumor volume significantly as compared to the control with MART-10 groups having more smaller tumor volume than $1\alpha,25(\text{OH})_2\text{D}_3$ group. **(c)** The tumor weights in both $1\alpha,25(\text{OH})_2\text{D}_3$ and MART-10 treated groups are lower than that in the control and MART-10 treated groups had the lowest tumor weight. **(d)** Serum calcium concentration in each group was steady. **(e)** No obvious change of body weight of mice was observed during the experiment period.

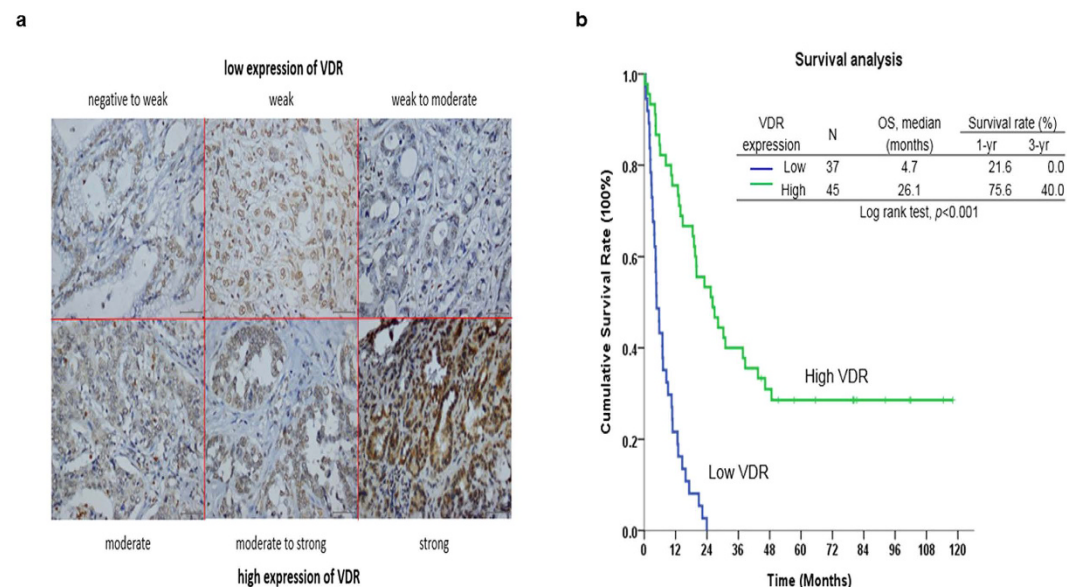


Figure 9. Immunohistochemical stain of VDR in human CCA specimen and the survival analysis of CCA patients based on VDR expression. **(a)** The different intensities of VDR expression in human CCA specimen. **(b)** Kaplan–Meier plot of overall survival in CCA patients undergoing hepatectomy based on their VDR expression levels. The low VDR expression group showed poorer overall survival ($P < 0.01$).

Another important physiological mechanism to maintain tissue homeostasis is apoptosis, which could remove unnecessary cells and curb unlimited proliferation⁴⁸. We investigated whether $1\alpha,25(\text{OH})_2\text{D}_3$ and MART-10

could induce apoptosis in CCA cells. Figure 3 demonstrates that neither $1\alpha,25(\text{OH})_2\text{D}_3$ nor MART-10 could induce CCA cells apoptosis as determined by TUNEL assay.

Human neutrophil gelatinase associated lipocalin (NGAL) has been reported to be expressed in malignant tumors arising from several organs^{49–51}. However, the role of NGAL in cancer is tissue-specific. In thyroid cancer, stable silencing of NGAL in thyroid cancer cells leads to a decrease in colony formation *in vitro* and decreased tumorigenicity and tumor size upon subcutaneous injection into nude mice⁵². However NGAL was shown to be involved in the growth and metastasis of endometrial cancer in humans⁵³. Regarding CCA, knockdown of NGAL has been shown to increase CCA cells invasiveness and doubling time^{28,54}. In addition, the serum NGAL levels were found to be significantly elevated in CCA patients compared to those with benign biliary tract disease⁵⁵. Our previous report further indicated that human CCA specimen presented with 66% high NGAL expression²⁸. Collectively, NGAL seems to play as an oncogene in human CCA. In this current study, to further verify NGAL role in CCA, the Ki-67 expression was measured in SNU308 cells and SNU308-NGALsi cells. As shown in Fig. 6c and d, SNU308-NGALsi cells has weaker Ki-67 expression than SNU308 cells, consistent with previous studies. As we treated SNU308 cells by $1\alpha,25(\text{OH})_2\text{D}_3$ and MART-10, NGAL expression was decreased with MART-10 more potent (Fig. 6a and b). The less growth inhibition effect of MART-10 and $1\alpha,25(\text{OH})_2\text{D}_3$ on SNU308-NGALsi cells as compared to SNU308 cells and rhNGAL could attenuate MART-10-induced growth inhibition in SNU308 and SNU308NGALsi cells further imply the growth inhibition effect of both drugs on SNU308 is partly mediated by downregulation of NGAL (Fig. 6e and f).

We then next investigated the role of VDR amid MART-10-induced inhibition of NGAL expression and cell growth in CCA cells. Figure 7b indicates that MART-10 repressed SNU308-VDRsi cell growth to a lesser extent as compared to that of SNU308 cells (Fig. 1b). The western blot and reporter assay demonstrated that the reporter activity and protein expression of NGAL in SNU308 cells were less influenced by MART-10 as VDR knockdown (Fig. 7c,d and e). Collectively, we concluded that MART-10 repressed CCA cell NGAL expression in a VDR dependent manner and VDR partly mediated MART-10-induced growth inhibition in CCA cells.

Since most genomic functions of $1\alpha,25(\text{OH})_2\text{D}_3$ are mediated by binding with VDR, we thus investigated VDR expression in human CCA specimens. Previously, Seubwai *et al.* had demonstrated that overexpression of VDR was a good indicator of prognosis for CCA patients²⁷. Supplemental Table 1 demonstrates that negative symptoms, negative lymph node metastasis and a negative resection margin were closely correlated with high VDR expression. Regarding OS, after multivariate Cox proportional hazard analysis, only low VDR staining intensity was identified as independent predictors for an inferior OS rate (Supplemental Table 2 and Fig. 8), in line with the previous study²⁷.

Conclusion

CCA is a devastating disease due to resistance to current available chemotherapies and radiotherapy and usually diagnosed late. MART-10, the newly synthesized $1\alpha,25(\text{OH})_2\text{D}_3$ analog, possesses potent anti-growth effect on CCA *in vitro* and *in vivo* without inducing obvious side effect. The finding that high expression of VDR is linked with better OS of CCA patients further implies the feasibility of application of vitamin D in CCA treatment. Collectively, further clinical trial of MART-10 application in CCA treatment is warranted.

Material and Method

Vitamin D compounds. $1\alpha,25(\text{OH})_2\text{D}_3$ was purchased from Sigma (St. Louis, MO, USA). MART-10 was synthesized as previously described²⁹.

Cell culture. SNU 308 and SNU1079 cells, human CCA cell lines, were obtained from Korean Cell Line Bank (KCLB: 28 Yongon-dong, Chongno-gu, Seoul 110–744, Korea). Cells were grown on RPMI 1640 medium supplemented with 10% FBS and 1% antibiotic-antimycotic agents. Culture medium was changed 3 times per week.

Cell proliferation assay by WST-1 kit. SNU 308 and SNU1079 cells were plated at about 1,000 cells per cm^2 in a 48-well cell culture cluster (Costar #3548, Corning Incorporated, Corning, NY, USA). Two days after the initial plating, the cells were treated with ethanol vehicle (control group) or $1\alpha,25(\text{OH})_2\text{D}_3$ or MART-10 at the indicated concentrations. The treatment was repeated 48 hours later. The viable cells were measured by WST-1 kits (Roche #11 644 807 001, Roche Diagnostics, GmbH, Mannheim, Germany) seven days after plating. The assay is based on the cleavage of the tetrazolium salt to formazan by cellular mitochondrial dehydrogenase.

Flow cytometry for cell cycle analysis. Cells were serum starved for 24 hours and then treated by indicated concentrations of $1\alpha,25(\text{OH})_2\text{D}_3$ or MART-10 for two days. Cells were then processed as previous described^{21,56}. Cell cycle analysis was performed using FACS-Calibur cytometer and CellQuestPro software (BD Biosciences, San Jose, CA); the data were analyzed using ModFit LT Mac 3.0 software.

Apoptosis analysis by Flow cytometry. After two days of $1\alpha,25(\text{OH})_2\text{D}_3$ or MART-10 treatment, cell apoptosis was analyzed using a flow cytometer with cells stained by APOTM-BrdU TUNEL kit. The operation procedures were according to the manufacturer's guideline.

Western blot analysis. The detailed procedures for western blot were described previously²¹. The primary antibodies used in this study were monoclonal antibodies against p21 (#2946, Cell Signal, Beverly, MA, USA.), p27 (#3698, Cell Signal), CDK4 (cell signal, #2906, Beverly, MA, USA), CDK6 (cell signal, #3136, Beverly, MA, USA), cyclin D3 (cell signal, #2936, Beverly, MA, USA), NGAL(#PAB9543, Abnova Corporation, Taipei, Taiwan). The secondary antibodies (1:5000) were anti-rabbit (111-035-003, Jackson ImmunoResearch, West

Grove, PA, USA) or anti-mouse secondary antibodies (Zymed 81–6520). The blots were detected using ECL reagents (WBKLS0500, Millipore, Billerica, MA, USA). Membranes were detected by VersaDoc™ Imaging System (Bio-Rad, Hercules, CA, USA) for analysis.

Knockdown of NGAL or VDR in SNU 308 cells. The procedures of knockdown of NGAL or VDR in SNU308 cells to obtain SNU308-NGALsi or SNU308-VDRsi cells were described previously²⁸.

Expression of Ki-67 antigen analyzed by flow cytometry. Two days after plating, SNU308 cells and SNU308-NGALsi cells were harvested by trypsin digestion and washed with PBS two times. The detailed procedures were described previously³³. The final pellets were incubated with Ki67 antibody and analyzed by flow cytometry.

Reporter Vector Constructs and Reporter Assay. One 7.9 kbp DNA fragment (+2514 to –5450) containing the 5′-flanking region of the human NGAL gene was isolated from the BAC clone (RP11–395P17; Invitrogen, Carlsbad, CA) digested with *Sac I*, and was subcloned into the pGEM3 vector (pGEM3_LCN2). The DNA fragment containing the enhancer/promoter of the NGAL gene (–5450 to +4) was synthesized with primers (T7 and 5′-CCATGGAGTGAGAGGCTCACCTGGGTGG-3′) by PCR using the pGEM3_LCN2 as target DNA, and was digested and cloned into the luciferase reporter vector (pGL3-Basic; Promega Biosciences) at the *Sac I* and *Nco I* sites. Proper ligation and orientation of the reporter vectors were confirmed by extensive restriction mapping and sequencing. The cells were plated onto 24-well plates at 1×10^4 cells/well 1 day prior to transfection. Cells were transiently transfected using the X-tremeGENE HP DNA transfection reagent (Roche Diagnostics, Indianapolis, IN) with 1 μg/well of reporter vector and 0.5 μg/well of the pCMVSPORTβgal (Invitrogen). The luciferase activity was adjusted for transfection efficiency using the normalization control plasmid pCMVSPORTβgal as previously described³⁷.

Animal study. Age-matched, non-obese, diabetic-severe, combined immunodeficient gamma (NOD.Cg-Prkdc^{scid} Il2rg^{tm1Wj}/SzJ JAX[®], NOD-SCID γ) male mice (8 weeks old, 20–25 g body weight) were used. 5×10^6 of SNU-308 cells were resuspended in 100 μL of PBS and injected into the subcutaneous. All animal experiments were conducted in accordance with a protocol approved by the Academia Sinica Institutional Animal Care and Utilization Committee (IACUC 14-03-665). One week after tumor injection, different treatment were started. Four groups were included in this study, i.e., ethanol treatment group as the shame group (twice per week, intraperitoneal injection, n = 6), 1α,25(OH)₂D₃ treatment group (0.3 ug/kg, twice per week, intraperitoneal injection, n = 6), MART-10 low-dose group (0.15 ug/kg, twice per week, intraperitoneal injection, n = 6), and MART-10 high-dose group (0.3 ug/kg, twice per week, intraperitoneal injection, n = 6). The tumor volumes, body weight and blood calcium were measured weekly. Tumor masses were harvested after 5 weeks. Blood calcium was measured using quantitative colorimetric calcium assay kits (BioChain, Newark, CA, USA) according to the manufacturer's protocol.

Patient demographics. We examined the demographic features of CCA 79 patients who underwent hepatectomy between 1989 and 2006 at the Department of Surgery of Chang Gung Memorial Hospital, Linkou, Taiwan. The study was approved by the local institutional review board of Chang Gung Memorial Hospital (clinical study numbers 99–2886B, 99–3810B and 102–5813B), and written informed consent for immunohistochemical tumor analysis was obtained from each patient. All methods relating to human experimentation were performed in accordance with the relevant guidelines and regulations.

VDR immunohistochemistry. VDR expression levels in the aforementioned 79 CCA patients were examined by immunohistochemical staining. Tissue sections (4-μm) prepared from the formalin-fixed, paraffin-embedded hepatectomy specimens were incubated with the primary antibody against VDR (MAB1360 1:1000 dilution; Millipore (Chemicon), USA) at 4 °C overnight. The detailed procedures were described previously²⁸. For the assessment of immunohistochemical staining, the percentage of stained target cells was evaluated in 10 random microscopic fields per tissue section (X400 magnification), and their averages were subsequently calculated. Staining intensities were scored as 1 (negative to weak), 2 (weak), 3 (weak to moderate), 4 (moderate), 5 (moderate to strong), or 6 (strong). Specimens with staining intensity scores of ≤3 or >3 were classified as having low or high expression, respectively.

Statistical analysis. For basic research, the data from each group were compared by unpaired t-test and p value < 0.05 was considered as a significant difference. For animal studies, Mann-Whitney U test was applied. For clinical research, numerical data was compared using independent Student's t-tests. Nominal data was compared using Pearson's χ^2 test or forward stepwise multiple logistic regression, as appropriate. Survival rate was calculated and plotted using the Kaplan-Meier method. Survival analysis was performed by using the log-rank test and multivariate analysis using the Cox proportional hazards model. SPSS statistical software program for Windows (SPSS version 10.0) was employed to conduct the statistics.

References

1. Alvaro, D. *et al.* Descriptive epidemiology of cholangiocarcinoma in Italy. *Dig Liver Dis* **42**, 490–495, doi: 10.1016/j.dld.2009.10.009 (2010).
2. Khan, S. A. *et al.* Guidelines for the diagnosis and treatment of cholangiocarcinoma: consensus document. *Gut* **51** Suppl 6, VII-9 (2002).
3. Taylor-Robinson, S. D. *et al.* Increase in mortality rates from intrahepatic cholangiocarcinoma in England and Wales 1968–1998. *Gut* **48**, 816–820 (2001).

4. Khan, S. A. *et al.* Changing international trends in mortality rates for liver, biliary and pancreatic tumours. *J Hepatol* **37**, 806–813, doi: S0168827802002970 (2002).
5. Gores, G. J. Cholangiocarcinoma: current concepts and insights. *Hepatology* **37**, 961–969, doi: 10.1053/jhep.2003.50200S0270913903002490 (2003).
6. Shaib, Y. & El-Serag, H. B. The epidemiology of cholangiocarcinoma. *Semin Liver Dis* **24**, 115–125, doi: 10.1055/s-2004-828889 (2004).
7. Casavilla, F. A. *et al.* Hepatic resection and transplantation for peripheral cholangiocarcinoma. *J Am Coll Surg* **185**, 429–436 (1997).
8. Ohtsuka, M. *et al.* Results of surgical treatment for intrahepatic cholangiocarcinoma and clinicopathological factors influencing survival. *Br J Surg* **89**, 1525–1531, doi: 2268 (2002).
9. Isaji, S. *et al.* Clinicopathological features and outcome of hepatic resection for intrahepatic cholangiocarcinoma in Japan. *J Hepatobiliary Pancreat Surg* **6**, 108–116, doi: 90060108.534 (1999).
10. Wang, Y. *et al.* Prognostic nomogram for intrahepatic cholangiocarcinoma after partial hepatectomy. *J Clin Oncol* **31**, 1188–1195, doi: 10.1200/JCO.2012.41.5984 (2013).
11. Fong, Y., Jarnagin, W. & Blumgart, L. H. Gallbladder cancer: comparison of patients presenting initially for definitive operation with those presenting after prior noncurative intervention. *Ann Surg* **232**, 557–569 (2000).
12. Burke, E. C. *et al.* Hilar Cholangiocarcinoma: patterns of spread, the importance of hepatic resection for curative operation, and a presurgical clinical staging system. *Ann Surg* **228**, 385–394 (1998).
13. Khan, S. A. *et al.* Guidelines for the diagnosis and treatment of cholangiocarcinoma: an update. *Gut* **61**, 1657–1669, doi: gutjnl-2011-301748 (2012).
14. Chiang, K. C. & Chen, T. C. The anti-cancer actions of vitamin D. *Anticancer Agents Med Chem* **13**, 126–139 (2013).
15. Feldman, D., Krishnan, A. V., Swami, S., Giovannucci, E. & Feldman, B. J. The role of vitamin D in reducing cancer risk and progression. *Nat Rev Cancer* **14**, 342–357, doi: 10.1038/nrc3691 (2014).
16. Deeb, K. K., Trump, D. L. & Johnson, C. S. Vitamin D signalling pathways in cancer: potential for anticancer therapeutics. *Nat Rev Cancer* **7**, 684–700, doi: 10.1038/nrc2196 (2007).
17. Leyssens, C., Verlinden, L. & Verstuyf, A. The future of vitamin D analogs. *Front Physiol* **5**, 122, doi: 10.3389/fphys.2014.00122 (2014).
18. Haussler, M. R. *et al.* The vitamin D hormone and its nuclear receptor: molecular actions and disease states. *J Endocrinol* **154** Suppl, S57–73 (1997).
19. Tsai, M. J. & O'Malley, B. W. Molecular mechanisms of action of steroid/thyroid receptor superfamily members. *Annu Rev Biochem* **63**, 451–486, doi: 10.1146/annurev.bi.63.070194.002315 (1994).
20. Ramagopalan, S. V. *et al.* A ChIP-seq defined genome-wide map of vitamin D receptor binding: associations with disease and evolution. *Genome Res* **20**, 1352–1360, doi: 10.1101/gr.107920.110 (2010).
21. Chiang, K. C. *et al.* 19-Nor-2 α -(3-hydroxypropyl)-1 α ,25-dihydroxyvitamin D₃ (MART-10) is a potent cell growth regulator with enhanced chemotherapeutic potency in liver cancer cells. *Steroids* **76**, 1513–1519, doi: 10.1016/j.steroids.2011.08.006 (2011).
22. Krishnan, A. V. & Feldman, D. Mechanisms of the anti-cancer and anti-inflammatory actions of vitamin D. *Annu Rev Pharmacol Toxicol* **51**, 311–336, doi: 10.1146/annurev-pharmtox-010510-100611 (2011).
23. Cross, H. S. & Kallay, E. Regulation of the colonic vitamin D system for prevention of tumor progression: an update. *Future Oncol* **5**, 493–507, doi: 10.2217/fon.09.22 (2009).
24. Welsh, J. Cellular and molecular effects of vitamin D on carcinogenesis. *Arch Biochem Biophys* **523**, 107–114, doi: S0003-9861(11)00356-0 (2012).
25. Chiang, K. C. *et al.* MART-10, a New Generation of Vitamin D Analog, Is More Potent than 1 α ,25-Dihydroxyvitamin D₃ in Inhibiting Cell Proliferation and Inducing Apoptosis in ER + MCF-7 Breast Cancer Cells. *Evid Based Complement Alternat Med* **2012**, 310872, doi: 10.1155/2012/310872 (2012).
26. Seubwai, W., Wongkham, C., Puapairoj, A., Okada, S. & Wongkham, S. 22-oxa-1,25-dihydroxyvitamin D₃ efficiently inhibits tumor growth in inoculated mice and primary histoculture of cholangiocarcinoma. *Cancer* **116**, 5535–5543, doi: 10.1002/cncr.25478 (2010).
27. Seubwai, W., Wongkham, C., Puapairoj, A., Khuntikeo, N. & Wongkham, S. Overexpression of vitamin D receptor indicates a good prognosis for cholangiocarcinoma: implications for therapeutics. *Cancer* **109**, 2497–2505, doi: 10.1002/cncr.22716 (2007).
28. Chiang, K. C. *et al.* Chemopreventive and chemotherapeutic effect of dietary supplementation of vitamin D on cholangiocarcinoma in a Chemical-Induced animal model. *Oncotarget* **5**, 3849–3861, doi: 10.18632/oncotarget.2000 (2014).
29. Ono, K. *et al.* Efficient synthesis of 2-modified 1 α ,25-dihydroxy-19-norvitamin D₃ with Julia olefination: high potency in induction of differentiation on HL-60 cells. *The Journal of organic chemistry* **68**, 7407–7415, doi: 10.1021/jo034787y (2003).
30. Chiang, K. C. *et al.* MART-10, a less calcemic vitamin D analog, is more potent than 1 α ,25-dihydroxyvitamin D₃ in inhibiting the metastatic potential of MCF-7 breast cancer cells *in vitro*. *J Steroid Biochem Mol Biol* **139**, 54–60, doi: 10.1016/j.jsbmb.2013.10.005 (2014).
31. Chiang, K. C. *et al.* MART-10, the vitamin D analog, is a potent drug to inhibit anaplastic thyroid cancer cell metastatic potential. *Cancer Lett* **369**, 76–85, doi: 10.1016/j.canlet.2015.07.024 (2015).
32. Chiang, K. C. *et al.* MART-10, the new brand of 1 α ,25(OH)₂D₃ analog, is a potent anti-angiogenic agent *in vivo* and *in vitro*. *J Steroid Biochem Mol Biol* **155**, 26–34, doi: 10.1016/j.jsbmb.2015.09.022 (2016).
33. Chiang, K. C. *et al.* MART-10, a novel vitamin D analog, inhibits head and neck squamous carcinoma cells growth through cell cycle arrest at G₀/G₁ with upregulation of p21 and p27 and downregulation of telomerase. *J Steroid Biochem Mol Biol* **138**, 427–434, doi: 10.1016/j.jsbmb.2013.09.002 (2013).
34. Chiang, K. C. *et al.* Topoisomerase inhibitors modulate gene expression of B-cell translocation gene 2 and prostate specific antigen in prostate carcinoma cells. *PLoS One* **9**, e89117, doi: 10.1371/journal.pone.0089117 (2014).
35. Chiang, K. C. *et al.* Evaluation of the potential therapeutic role of a new generation of vitamin D analog, MART-10, in human pancreatic cancer cells *in vitro* and *in vivo*. *Cell Cycle* **12**, 1316–1325, doi: 10.4161/cc.24445 (2013).
36. Flower, D. R. The lipocalin protein family: structure and function. *Biochem J* **318** (Pt 1), 1–14 (1996).
37. Yang, J. *et al.* An iron delivery pathway mediated by a lipocalin. *Mol Cell* **10**, 1045–1056 (2002).
38. Candido, S. *et al.* Roles of neutrophil gelatinase-associated lipocalin (NGAL) in human cancer. *Oncotarget* **5**, 1576–1594, doi: 10.18632/oncotarget.1738 (2014).
39. Lim, R. *et al.* Neutrophil gelatinase-associated lipocalin (NGAL) an early-screening biomarker for ovarian cancer: NGAL is associated with epidermal growth factor-induced epithelio-mesenchymal transition. *Int J Cancer* **120**, 2426–2434, doi: 10.1002/ijc.22352 (2007).
40. Tong, Z. *et al.* Neutrophil gelatinase-associated lipocalin: a novel suppressor of invasion and angiogenesis in pancreatic cancer. *Cancer Res* **68**, 6100–6108, doi: 10.1158/0008-5472.CAN-08-0540 (2008).
41. Lee, H. J. *et al.* Ectopic expression of neutrophil gelatinase-associated lipocalin suppresses the invasion and liver metastasis of colon cancer cells. *Int J Cancer* **118**, 2490–2497, doi: 10.1002/ijc.21657 (2006).
42. Saito, N., Honzawa, S. & Kittaka, A. Recent results on A-ring modification of 1 α ,25-dihydroxyvitamin D₃: design and synthesis of VDR-agonists and antagonists with high biological activity. *Curr Top Med Chem* **6**, 1273–1288 (2006).

43. Iglesias-Gato, D. *et al.* Substitution at carbon 2 of 19-nor-1 α ,25-dihydroxyvitamin D₃ with 3-hydroxypropyl group generates an analogue with enhanced chemotherapeutic potency in PC-3 prostate cancer cells. *J Steroid Biochem Mol Biol* **127**, 269–275, doi: S0960-0760(11)00169-5 (2011).
44. Flanagan, J. N. *et al.* Evaluation of 19-nor-2 α -(3-hydroxypropyl)-1 α ,25-dihydroxyvitamin D₃ as a therapeutic agent for androgen-dependent prostate cancer. *Anticancer Res* **29**, 3547–3553, doi: 29/9/3547 (2009).
45. Malumbres, M. & Barbacid, M. Cell cycle, CDKs and cancer: a changing paradigm. *Nat Rev Cancer* **9**, 153–166, doi: 10.1038/nrc2602 (2009).
46. Krtolica, A., Krucher, N. A. & Ludlow, J. W. Hypoxia-induced pRB hypophosphorylation results from downregulation of CDK and upregulation of PP1 activities. *Oncogene* **17**, 2295–2304, doi: 10.1038/sj.onc.1202159 (1998).
47. Powers, J. T. *et al.* E2F1 uses the ATM signaling pathway to induce p53 and Chk2 phosphorylation and apoptosis. *Mol Cancer Res* **2**, 203–214 (2004).
48. Elmore, S. Apoptosis: a review of programmed cell death. *Toxicol Pathol* **35**, 495–516, doi: 10.1080/01926230701320337 (2007).
49. Mallbris, L. *et al.* Neutrophil gelatinase-associated lipocalin is a marker for dysregulated keratinocyte differentiation in human skin. *Experimental dermatology* **11**, 584–591 (2002).
50. Bauer, M. *et al.* Neutrophil gelatinase-associated lipocalin (NGAL) is a predictor of poor prognosis in human primary breast cancer. *Breast cancer research and treatment* **108**, 389–397, doi: 10.1007/s10549-007-9619-3 (2008).
51. Cho, H. & Kim, J. H. Lipocalin2 expressions correlate significantly with tumor differentiation in epithelial ovarian cancer. *The journal of histochemistry and cytochemistry: official journal of the Histochemistry Society* **57**, 513–521, doi: 10.1369/jhc.2009.953257 (2009).
52. Iannetti, A. *et al.* The neutrophil gelatinase-associated lipocalin (NGAL), a NF- κ B-regulated gene, is a survival factor for thyroid neoplastic cells. *Proceedings of the National Academy of Sciences of the United States of America* **105**, 14058–14063, doi: 10.1073/pnas.0710846105 (2008).
53. Miyamoto, T. *et al.* Laser-captured microdissection-microarray analysis of the genes involved in endometrial carcinogenesis: stepwise up-regulation of lipocalin2 expression in normal and neoplastic endometria and its functional relevance. *Human pathology* **42**, 1265–1274, doi: 10.1016/j.humpath.2010.07.027 (2011).
54. Nuntagawat, C., Leelawat, K. & Tohtong, R. NGAL knockdown by siRNA in human cholangiocarcinoma cells suppressed invasion by reducing NGAL/MMP-9 complex formation. *Clinical & experimental metastasis* **27**, 295–305, doi: 10.1007/s10585-010-9327-y (2010).
55. Leelawat, K., Narong, S., Wannaprasert, J. & Leelawat, S. Serum NGAL to Clinically Distinguish Cholangiocarcinoma from Benign Biliary Tract Diseases. *International journal of hepatology* **2011**, 873548, doi: 10.4061/2011/873548 (2011).
56. Ouyang, W. *et al.* Cyclin D1 induction through I κ B kinase beta/nuclear factor- κ B pathway is responsible for arsenite-induced increased cell cycle G1-S phase transition in human keratinocytes. *Cancer Res* **65**, 9287–9293, doi: 65/20/9287 (2005).
57. Tsui, K. H. *et al.* Prostate-derived ets factor represses tumorigenesis and modulates epithelial-to-mesenchymal transition in bladder carcinoma cells. *Cancer Lett* **375**, 142–151, doi: 10.1016/j.canlet.2016.02.056 (2016).

Acknowledgements

This work is supported by 103-2314-B-182A-085 -, 104-2314-B-182A-017 – and 105-2314-B-182A-046- (belong to ministry of science and technology) CMRPG2D0191, 0192 and 0193 (belong to Chang Gung memorial hospital) to Kun-Chun Chiang; NMRPG5D6031, NMRPG5D6032, MOST103-2314-B-182A-081-MY2, and CMRPG3E1611 to Chun-Nan Yeh.

Author Contributions

K.-C.C. wrote the manuscript and designed this experiment. T.-S.Y. wrote the manuscript and designed this experiment. C.-C.H. helped conduct the experiment. Y.-C.C. helped conduct the experiment. J.-H.P. helped conduct the experiment. J.-T.H. helped conduct the experiment. C.-T Cheng conducted statistics. M.T. created the compound. A.K. created the compound. T.-C.C. helped review the article. H.H.J. in charge of the whole experiment conduction. M.H. was in charge of the whole experiment conduction. C.-N.Y. was in charge of the whole experiment conduction and paper writing.

Additional Information

Supplementary information accompanies this paper at <http://www.nature.com/srep>

Competing Interests: The authors declare no competing financial interests.

How to cite this article: Chiang, K.-C. *et al.* MART-10 represses cholangiocarcinoma cell growth and high vitamin D receptor expression indicates better prognosis for cholangiocarcinoma. *Sci. Rep.* **7**, 43773; doi: 10.1038/srep43773 (2017).

Publisher's note: Springer Nature remains neutral with regard to jurisdictional claims in published maps and institutional affiliations.



This work is licensed under a Creative Commons Attribution 4.0 International License. The images or other third party material in this article are included in the article's Creative Commons license, unless indicated otherwise in the credit line; if the material is not included under the Creative Commons license, users will need to obtain permission from the license holder to reproduce the material. To view a copy of this license, visit <http://creativecommons.org/licenses/by/4.0/>

© The Author(s) 2017